World Academy of Science, Engineering and Technology
International Journal of Industrial and Manufacturing Engineering
Vol:5, No:1, 2011

Operation Assay of an Industrial Single-Source – Single-Detector Gamma CT Using MCNP4C Code Simulation and Experimental Test Comparisons

M. Ghanadi, M. Rezazadeh*, M. Ardeshiri, R. Gholipour Peyvandi, M. Jafarzadeh, M. Shahriari, M.Rezaei Rad, Z. Gholamzadeh

***Abstract*—**A 3D industrial computed tomography (CT) manufactured based on a first generation CT systems, single-source – single-detector, was evaluated. Operation accuracy assessment of the manufactured system was achieved using simulation in comparison with experimental tests. ^{137}Cs and ^{60}Co were used as a gamma source. Simulations were achieved using MCNP4C code. Experimental tests of ^{137}Cs were in good agreement with the simulations

***Keywords*—**Gamma source, Industrial CT, MCNP4C, Operation assessment.

I. Introduction

NUCLEAR imaging systems, such as gamma computed tomography, are used to analyze and identify failures in industrial processes and permitting to visualize failure points in three-dimensional analysis [1]-[2].

Computed tomography is a noninvasive imaging technique that has been used extensively in not only medicine diagnosis and surgical planning, but also in nondestructive testing (NDT) for many industrial applications such as mechanical part manufacturing, production of composite materials, waste container inspection, metrology, detection of structural defects and others, heterogeneities in polymer objects, and so on. The current industrial CT technology is capable of generating very high-resolution images [4]-[10].

Most industrial CT was used X-ray sources. Nonetheless, gamma-ray CT has many advantages over X-ray CT in the diagnosis of large-scale industrial process units. The X-rays produced in common X-ray tubes have a broad energy spectrum. It is therefore desirable to provide an efficient imaging system having monoenergetic X-ray or γ-ray source.

Gamma-ray sources provide a highly penetrating fan beam of single energy gamma rays. These gamma rays have a much higher effective energy than commonly used X-ray sources [11].

Tomographic imaging consists of directing γ-rays at an object from multiple orientations and measuring the decrease in intensity along a series of linear paths.

M. Ghanadi is with Nuclear Science and Technology Research Institute,Iran,e-mail:m_rezazadeh14@yahoo.com

This decrease is characterized by Beer's Law, which describes intensity reduction as a function of γ-ray energy, path length, and linear attenuation coefficient of material. A specialized algorithm is then used to reconstruct the distribution of γ-ray attenuation in the volume being imaged [12].

Hence, a home-made manufactured single-source & single-detector 3D gamma-ray CT system was used in this work to evaluate: 1- the system mechanical errors, 2- effects of utilizing different single-energy sources on the acquired image, and 3- comparing experimental and simulations.

II. MATRIAL And Method

A. Sestem setup

To set accurate and precise position of a phantom, three motors were used. Two three-phase motors (Three-phase, 0.22 kW power, MarelliMotori Company, MA 63 MB 4 technical code) with 1800 rpm speed were used to adjust R and Z positions of the phantom and one DC motor (24 V DC, Hitachi brand) set θ position of the phantom. Each motor speed was adjusted by inventor and microprocessor combination (frequency converter, HYUNDAI Company, N50 model, 1-60 Hz velocity range). θ position was declared by an encoder (13-bit, 6FX2001-5FS12 model, Siemens Company). Position accuracy of the phantom according to a prior determined position control using 0.01 mm precision digital calipers (0-500 mm, 6FX2001 model, Guanglu Company) mounted for R and Z orientations. An AVR microcontroller (model 128 Atmega, Atmel Company) was used to adjust the phantom position with 0.01 mm precision. To match electronic zero and mechanical zero, an optostop was used. Also some limiting microswitches ensure more apparatus custody. Digital position-measurement system was used in the manner that cheap commercial digital caliper output will be readable for microcontroller by using an interface circuit. The mentioned apparatus was applied to report accurate position in Z and R orientations. Phantom holder board was designed so that could bear 30 Kg maximum weight. Maximum phantom dimensions are a cylinder of 270 mm diameter and 200 mm height related to minimum and maximum range limitations.

Nuclear electronic system consist of a NaI(Tl) (2×2, model 905-3 , ORTEC company), and a specialized MCA (model 166) consist of pre-amplifier, amplifier, high voltage (HV) and a data acquisition system .

Two cylindrical lead collimators were used for source and detector (Detector collimator; inner diameter: 0.5 cm, outer diameter: 10.4 cm, usable height: 13.4cm, Source collimator; inner diameter: 0.5 cm, outer diameter: 10.4 cm, position of sitting source: 6 cm.) A schematic design of system has been show is Fig. 1. ^{137}Cs (30 mCi) and ^{60}Co (5.6 mCi) was used as a gamma source for the designed single-source – single-detector industrial CT system. The intensity of transmitted gamma rays was calculated using peak area.

B. Design of Phantoms

Two polyethylene ($\rho = 0.94\,g/cm^3$) phantoms named P10-1 and P10-2 were used to carry out assessment tests of the system operation. P10-1 cylindrical phantom was made of polyethylene having 103 mm diameter and 80 mm height containing five aluminum ($\rho = 2.7\,g/cm^3$) rods (rods' diameter: 3.5, 5.5, 8.0, 10 and 14.8 mm) improvised into it. P10-2 polyethylene cylindrical of 105 mm diameter and 80 m height containing holding five air ($\rho = 0.00129\,g/m^3$) holes instead of the aluminum rods (holes' diameter: 5, 6.5, 8.5, 10.5 and 13.0 mm) holding five air ($\rho = 0.00129\,g/m^3$) holes instead of the aluminum rods. A polyethylene phantom was used to determine the 2D imaging quality of the designed industrial CT system. The phantom was made as cylindrical geometry that 12 holes of 1.5, 2, 2.5, 3 mm in diameter was improvised on a inner ring and 3, 5, 7, 9, 11, 15, 16 and 17 mm diameters was improvised on a outer ring.

C. Simulation and Experimental Comparison

Before outset of experimental tests, it is mandatory to be determined if mechanical errors are in imaging direction such as phantom shift concluded incorrect operation of the digital caliper and so. Hence, several similar 1D imaging were repeated.

1D imaging of the polyethylene phantoms using two ^{137}Cs & ^{60}Co source and the NaI detector was simulated via MCNP4C code [13]. Source, geometry and materials were defined with respect to experimental setup and the response of detector was determined using tally F8 in MCNP4C code. These tallies are pulse height tally and produce the response function of gamma detector. The FWHM of peak was applied by FT8 card joined to F8 tally card. Iron rods were riveted on the phantom holder board as indicators that identify edges of the rested phantom on the board center. Experimental data collecting was carried out via counting net area as follow (1):

$$Area = Integral - Background \tag{1}$$

$$Integral = \sum_{i=RoI_{begin}}^{RoI_{end}} spectrum_i$$

$$Background = \frac{RoI_{end} - RoI_{begin}}{8} \times \left(\sum_{i=RoI_{begin-s}}^{RoI_{begin}} spectrum_i - \sum_{i=RoI_{end}}^{RoI_{end+s}} spectrum_i \right)$$

That ROI was chosen as follow: 564.94-756.69 keV for ^{137}Cs and 1086.45-1251.19 keV & 1251.19 1413.96 keV for ^{60}Co peaks.

I/I_0 make image that I_0 is entrance photon on phantom surface and I is output photon of the phantom.

The validity of the manufactured CT scanner was achieved using MCNP4C-based Monte Carlo simulator relative difference between simulative and experimental results has been evaluated by (2):

$$NE = \frac{Measured - Simulated}{Measured} \tag{2}$$

A 1mm steps was chosen to scan the phantoms. The scans were carried out in alignment axis of the holes.

III. Results and Discussion

A. Mechanical errors

To find any mechanical errors, scan of the five-hole polyethylene phantoms (ph10-1 and ph10-2) were carried out in twice at constant condition (1-1 & 1-2 tests). Another scan was carried in against direction using the similar condition of two prior tests (2-1 test). Relation errors showed an acceptable mechanical error of less than 1.8% (Fig. 2).

B. Comparison of ^{137}Cs & ^{60}Co 1D simulation

Simulation calculations for Ph10-1 & Ph10-2 showed high energy don't seems to be suitable for dense materials. In case of ^{60}Co simulation, boundaries of air and polyethylene are sharper than ^{137}Cs (Fig. 3).

C. Comparison between simulations – experimental results

The Ph10-1 simulation and the experimental test comparison using ^{137}Cs showed there are 5.48% average relative errors respectively (Fig. 4,5,6,7). The phantom tomography by means of ^{137}Cs showed that its acquired projection behavior, except 3.5 mm hole is similar to the simulated results. 2D imaging of the polyethylene phantom of 12 air holes was formed. Unprocessed image is shows in Fig. 8 With respect to this result the resolution of system is 5 mm and smaller holes were not shows in image.

IV. Conclusion

Simulations using MCNP-4C suggests ^{137}Cs as more useful source than ^{60}Co. The experimental tests using ^{137}Cs source showed good ability of the designed industrial CT for imaging with mechanical errors less 1.8%. The system has desirable ability to detect a 5 mm hole in 2D imaging.

REFERENCES

[1] J., Noel, "Advantages of CT in 3D Scanning of Industrial Parts" , *North Star Imaging Inc.* 1(3) (2008)18.

[2] J.M., de Oliveira Jr., A.C.G., Martins and J.A., DE Milito, "Analysis of Concrete Material through Gamma Ray Computerized Tomography", *Brazilian Journal of Physics* A 34(3) (2004) 1020.

[3] H. Toyokawa et al., "Gamma-ray computed tomography using 10 MeV laser-compton photon beam", *Proceedings of the Particle Accelerator Conference*. (2003) .

[4] W.A.P., Calvo et al., "Gamma-ray computed tomography SCANNERS for applications in multiphase system columns", *NUKLEONIKA*. 54(2) (2009)129 .

[5] D.C., Camp, H.E., Martz, G.P., Roberson, D.J., Decman and R.T., Bernardi, "Nondestructive waste-drum assay for transuranic content by gamma-ray active and passive computed tomography", *Nuclear Instruments and Methods in Physics Research Section A: Accelerators, Spectrometers, Detectors and Associated Equipment*. 495(1) (2002) 69.

[6] H.,Lettenbauer, B. Georgi and D. Weiß, "Means to Verify the Accuracy of CT Systems for Metrology Applications", (In the Absence of Established International Standards) DIR 2007 - *International Symposium on Digital industrial Radiology and Computed Tomography*, Lyon, France, (2007).

[7] D., Braz, R.T., Lopes and L.M.G., da Motta, "Computed tomography: an evaluation of the effect of adding polymer SBS to asphaltic mixtures used in paving" , *Applied Radiation and Isotopes*. 53(4-5) (2000) 725.

[8] M.C., Rocha et al., "Moisture profile measurements of concrete samples in vertical water flow by gamma ray transmission method", *Radiation Physics and Chemistry*. 61(3) (2001) 567.

[9] A., Rinnhofer, A. Petutschnigg and J.-P., Andreu, "Internal log scanning for optimizing breakdown", *Computers and Electronics in Agriculture*. 41(1-3) (2003) 7.

[10] Flisch, A. et al, "Industrial Computed Tomography in Reverse Engineering Applications". *DGZfPProc*. BB 67-CD. (1999)8.

[11] L., Franco, F., Gómez, A., Iglesias, F., Vidal and R., "Ameneiro, Industrial radiography and tomography based on scanning linear scintillator array". *4th international conference on NDT. Ceret Greece.* (2007).

[12] "Industrial process gamma tomography": final report of a coordinated research project (IAEA-TECDOC 1589) by *International Atomic Energy Agency* (2003-2007).

[13] Briesmeister, J., 2000. "MCNPTM—a general Monte Carlo NParticle Transport Code", LA 1265-M, Version 4C. Los Alamos Laboratory, USA.

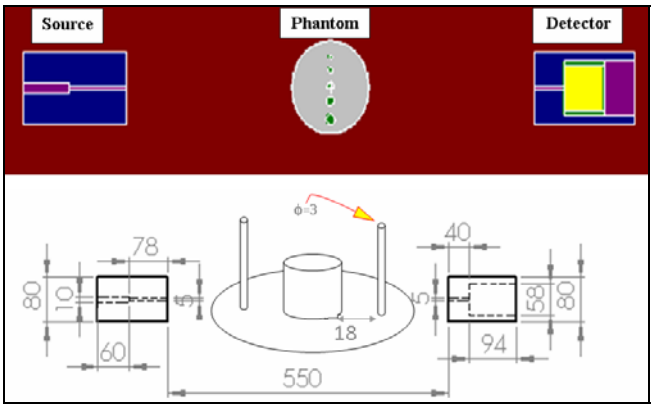

Fig. 1 Schematic design of placing phantom on phantom holder board between the shielded source and detector.

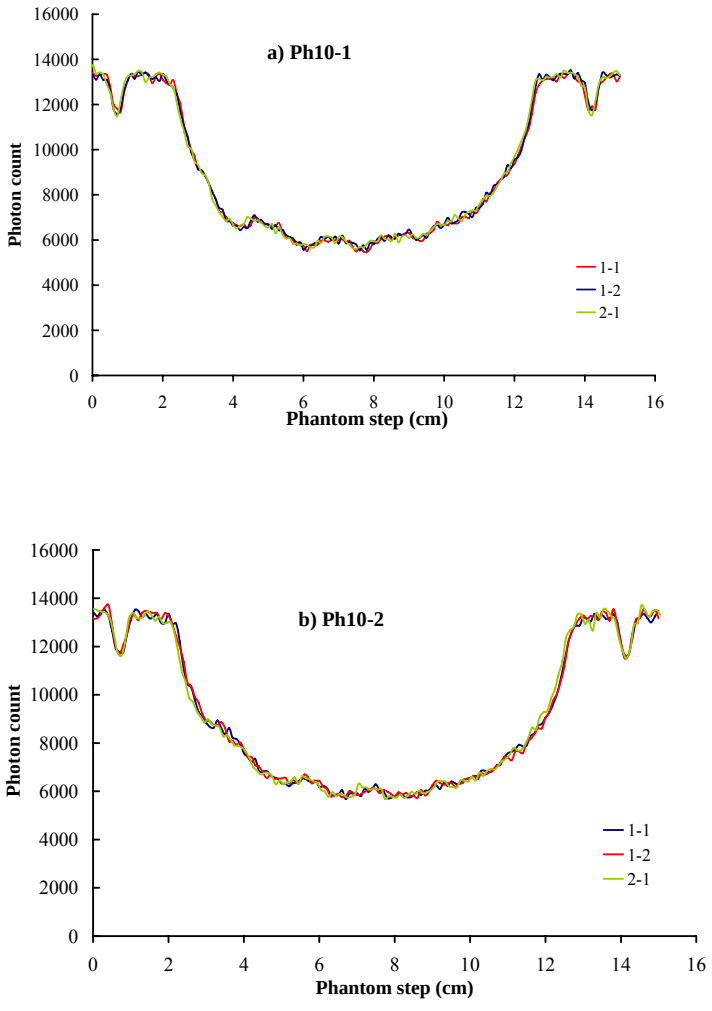

Fig. 2 Evaluation of mechanical errors using source Cs-137 and .the phantom a) aluminum rods (ph10-1), rods' diameter : 3.5, 5.5, 8.0, 10 and 14.8 mm , b) air holes (ph10-2), holes' diameter: 5, 6.5, 8.5, 10.5 and 13.0 mm .

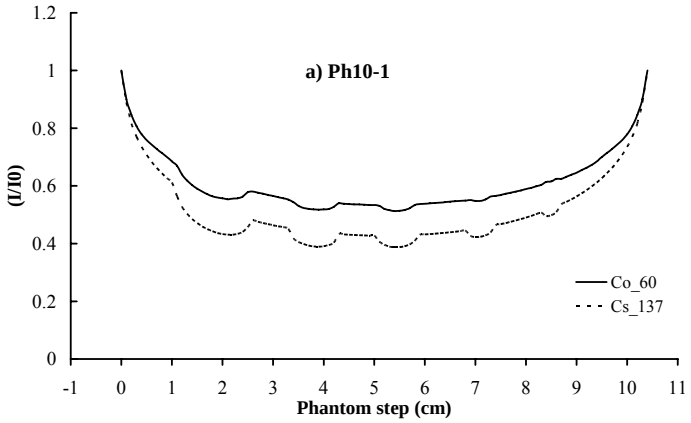

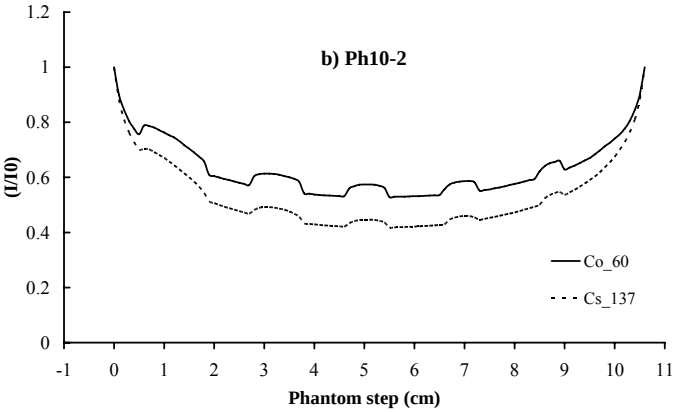

Fig. 3 Comparison of Cs-137 and Co-60 source via imaging of the phantom a) aluminum rods (ph10-1), rods' diameter: 3.5, 5.5, 8.0, 10 and 14.8 mm , b) air holes (ph10-2), holes' diameter: 5, 6.5, 8.5, 10.5 and 13.0 mm .

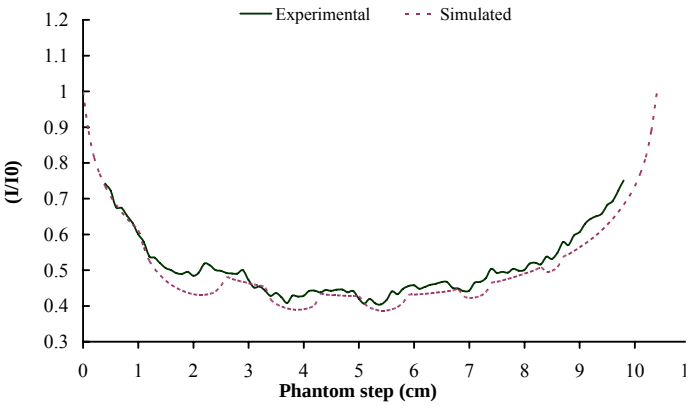

Fig. 4 Comparison of experimental and simulation using Cs-137 source for phantom with aluminum rods (ph10-1), rods' diameter: 3.5, 5.5, 8.0, 10 and 14.8 mm .

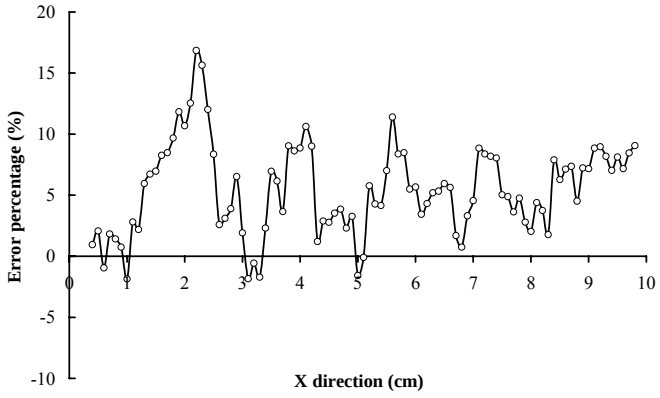

Fig. 5 Relative error determination of ph10-1 imaging via Cs-137 source

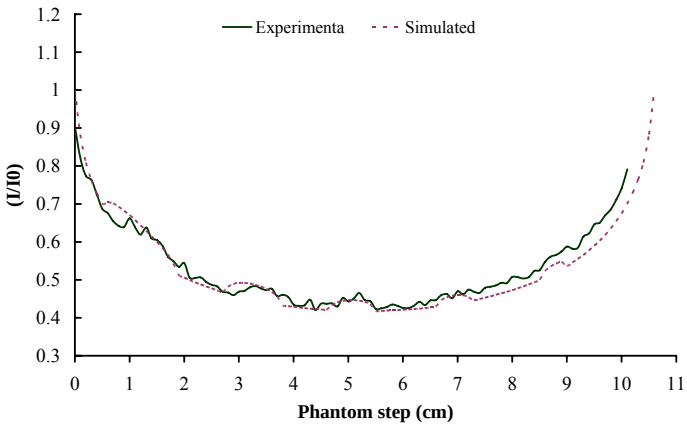

Fig. 6 Comparison of experimental and simulation using Cs-137 source for phantom air holes (ph10-2), holes' diameter: 3.5, 5.5, 8.0, 10 and 14.8 mm .

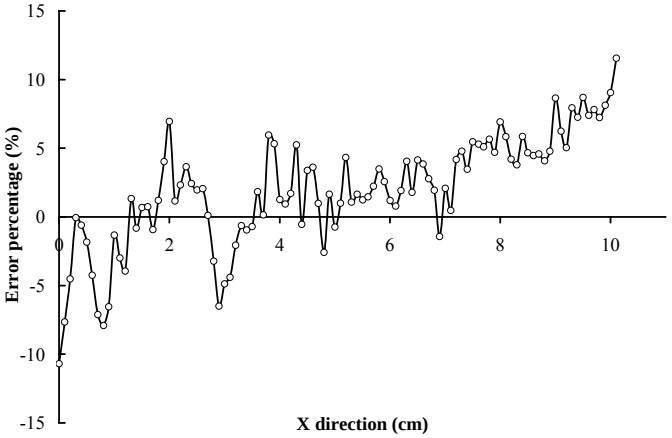

Fig. 7 Relative error determination of ph10-2 imaging via Cs-137 source

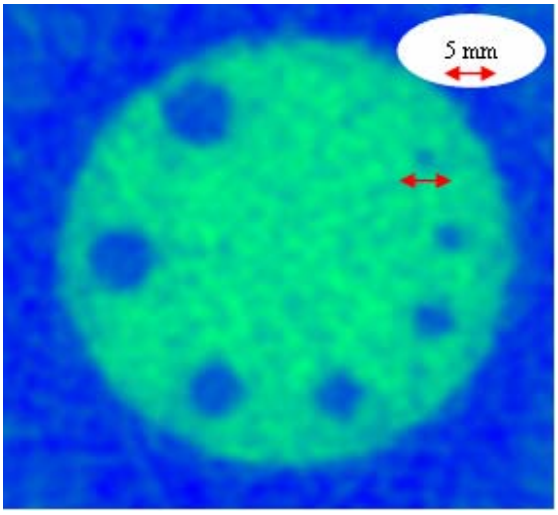

Fig. 8 Polyethylene phantom 2D image, air holes, minimum resolution: 5mm, θ: 356.4˚, Δθ: 4.39˚, ΔR: 1.2 mm, Time/Sample: 10 s, source - detector distance: 55 cm.

TABLE I
GAMMA CT PARAMETERS DURING IMAGING

High Voltage	669-711 Volt
Lower Level	1.5 or 3
Coarse Gain	40
Fine Gain	7.5-9
Peak Width	5
Peak Search Sensitivity	3